In Situ Study of Size and Temperature Dependent Brittle-to-Ductile Transition in Single Crystal Silicon

*Wonmo Kang, and M. Taher A. Saif**

Silicon based micro- and nanometer scale devices operating at various temperatures are ubiquitous today. However, thermo-mechanical properties of silicon at the small scale and their underlying mechanisms remain elusive. The brittle-to-ductile transition (BDT) is one such property relevant to these devises. Materials can be brittle or ductile depending on temperature. The BDT occurs over a small temperature range. For bulk silicon, the BDT is about 545 °C. It is speculated that the BDT temperature of silicon may decrease with size at the nanoscale. However, recent experimental and computational studies have provided inconclusive evidence, and are often contradictory. Potential reasons for the controversy might originate from the lack of an in situ methodology that allows variation of both temperature and sample size. This controversy is resolved in the present study by carrying out in situ thermo-mechanical bending tests on single crystal silicon samples with concurrent control of these two key parameters. It is unambiguously shown that the BDT temperature reduces with sample size. For example, the BDT temperature decreases to 293 °C for a sample size 720 nm. A mechanism-based model is proposed to interpret the experimental observations.

1. Introduction

Micro/nanomaterials exhibit significantly different mechanical behavior from their bulk counterparts.[1–8] Several fundamental mechanisms for the size dependent material behavior have been reported in the literature including dislocation pile-up (Hall–Petch behavior,[3,4] dislocation starvation,[7] and microstructural heterogeneity.[6] In addition, strain-gradient-dependent strengthening was observed among small scale metal samples during nanoindentation,[5] bending,[9] and torsion[10] tests.

Size dependent material properties of brittle semiconductive materials such as Si and SiC have received attention due to their extensive use in micro-/nanometer scale devices. In many cases, the small scale systems are required to operate at high temperatures, e.g., in microturbines,[11] micropower generators[12] and sensors/actuators[13] in automobile and aerospace applications. Hence, accurate characterization of thermo-mechanical properties and understanding of fundamental mechanism in materials deformation are essential as plastic deformation can lead to substantial change in electrical and mechanical responses of materials.

One thermo-mechanical property of materials, with the exception of FCC metals, is that they are brittle at low temperature, but become ductile at higher temperature. This brittle to ductile transition (BDT) occurs over a narrow range of temperature, referred to as the BDT temperature. The BDT temperature is determined through fracture experiments. Fracture toughness, which offers an indirect measure of the degree of plasticity ahead of a crack tip, increases rapidly at the BDT. For single crystal silicon (SCS), the sudden increase in fracture toughness occurs in the range 541–545 °C.[14] The underlying micromechanism for BDT is a large increase in dislocation density and their increased mobility with temperature,[15] which facilitates plastic deformation under stress. The temperature range over which this transition occurs depends on the initial defect density. For example, steel with high bulk defect density shows gradual transition over tens of degrees below room temperature[16] while transition occurs within a few degrees for SCS at 545 °C.[14]

Is BDT temperature size dependent? There are limited but conflicting reports in the literature on the BDT temperature of SCS. Nakao et al.[17] carried out three point bending tests directly on a hot plate by using micrometer scale SCS samples (4 μm in thickness) with a notch and observed significant reduction in the BDT temperature. The fracture toughness increased rapidly as the temperature approached 70 °C. Their postmortem observation of the fractured surface in SEM revealed that the BDT is triggered by a rapid increase in dislocation density.

Han et al.[18] reported ductile deformation in SCS nanowires with diameter less than 60 nm at room temperature, tested in situ in TEM. Östlund et al[19] carried out micropillar compression tests with a variation in sample diameter and observed ductility in samples with size less than ≈300–400 nm at room temperature. These experiments imply that submicrometer-sized SCS undergoes BDT below room temperature. However, Zhu et al.[20] tested SCS nanowires by uniaxial tension at room temperature where no ductility was observed even for nanowires 16 nm in diameter. The authors argued that the large plastic deformation reported in the work of Han et al.[18] might be due to strong electron beam irradiation during TEM observation. Bending tests of 255-nm-thick silicon beams,[21]

Dr. W. Kang, Prof. M. T. A. Saif
Department of Mechanical Science and Engineering
University of Illinois
1206 W. Green St., Urbana, IL 61801, USA
E-mail: saif@illinois.edu

DOI: 10.1002/adfm.201201992

and silicon nanowires with diameters between 200–300 nm[22] did not show any plastic deformation at room temperature. These experiments imply that submicrometer-sized SCS samples have a BDT above room temperature. Note that the measured bending strengths were 17.53 GPa (200 nm in width) in Ref.[21] and 18.3 GPa (120 nm in diameter) in Ref.[22] while the yield stress for 250 nm SCS micropillars under compression in Ref.[19] was ≈2.5–4 GPa at room temperature. With the exception of fracture tests, all of the above studies were carried out at room temperature. The sample size was changed in search of a small enough size that will undergo BDT at room temperature.

In this paper, we vary both the temperature and the sample size using a novel method developed by Kang and Saif.[23,24] We hypothesize that the BDT temperature decreases with sample size due to increased surface to volume ratio. In order to test our hypothesis, we carry out in situ bending test on SCS beams with widths of 720 nm to 8.7 μm from room temperature to 375 °C. We find a significant reduction in the BDT temperature with a reduction in sample size. In the following section, we briefly introduce the novel, in situ thermo-mechanical testing method. We then present the load-deformation relationships of the SCS bending samples with increasing in temperature. The results show a reduction in the BDT temperature up to 31.2% with respect to the bulk BDT temperature. We propose a model to explain the relationship between the sample size and the reduced BDT temperature.

2. Experimental Section

2.1. Challenges for In Situ Material Testing

Ultrahigh resolution electron microscopy observation allows quantitative, in situ testing of micro/nanomaterials by providing a direct structure-property relationship.[25–28] However, in situ thermo-mechanical characterization of micro/nanoscale samples involves several challenges including (i) fabrication, handling, and gripping of the small samples, (ii) limited available space in analytical chambers, and (iii) in situ heating of a sample with quantitative temperature measurement. In addition, large variations in temperature impose unavoidable challenges in loading the sample. For example, a stage and sample can have different thermal expansion coefficients, which may cause undesired loading/unloading of a sample with variation of temperature. In order to overcome these challenges and to carry out in situ thermo-mechanical testing of SCS at micrometer and nanometer scale, we use a novel SiC based MEMS apparatus which allows independently testing of the fabricated micro/nanoscale samples with concurrent control of sample size and temperature.[23,24]

2.2. A Microdevice for Thermo-Mechanical Measurement

A novel SiC MEMS stage for in situ thermo-mechanical testing is shown in **Figure 1**a. The overall size of the stage is small enough to perform in situ SEM and TEM material tests. As described elsewhere,[29,30] the stage has two grooves at Area C in Figure 1a which serve as grips for a bending sample and hence the stage can be used to test independently fabricated samples without limitation on sample dimensions and materials. Figure 1b,c show a SCS bending sample after assembly of the stage by a micromanipulator. The sample is loaded by deforming the stage using a piezoelectric actuator as described elsewhere.[29,30] Beams at A-A and B-B in Figure 1a serve as a support and a force sensor for the sample, respectively. Upon mechanical loading, the support springs, A-A, transfer the deformation to the sample. SEM images are taken to measure deformation of the sample and the force sensing beams with precalibrated known stiffness. The SEM images are analyzed

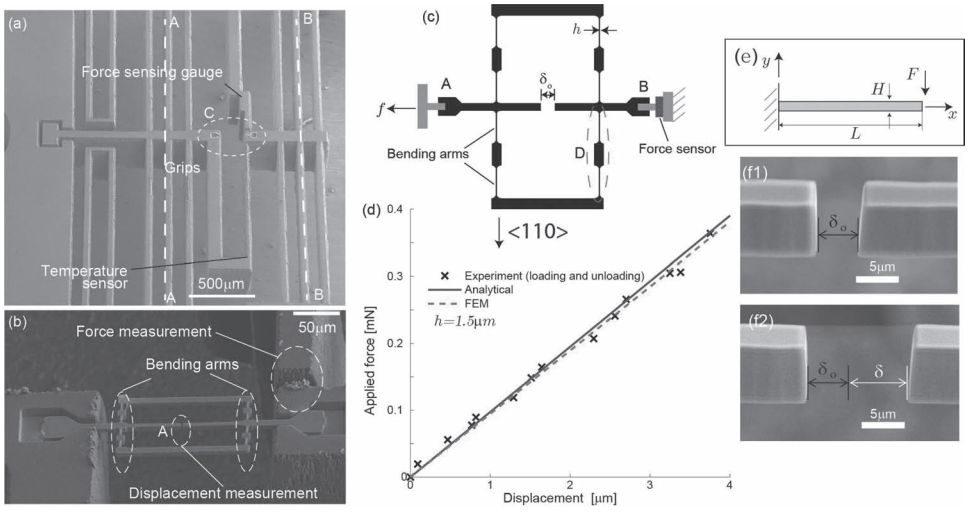

Figure 1. Experimental method for in situ thermo-mechanical test. a) SEM image of the MEMS stage for in situ test. Reproduced with permission.[24] Copyright 2011, Institute of Physics Publishing. b) Zoom-in view (Area C) of the silicon bending sample on the MEMS stage. c) Schematic of the bending sample. d) Force-displacement relationship, and (f1)-(f2) zoom-in view of Area A in (b). During in situ testing, the sample displacement (δ) and applied force (f) are measured by analyzing high resolution SEM images, as shown in (d). Displacement measurements are conducted without exposing the bending arms to the electron beam during in situ testing by measuring at a position away from the bending arms (Area A in (b)).

with a correlation algorithm (Matlab) for automated image tracking with enhanced tracking resolution. As mentioned earlier, the effect of electron beam irradiation on the size dependent BDT in SCS is still not conclusive.[18,20] Hence, we did not expose the bending arms to the electron beam during in situ experiments to avoid possible effects of electron beam irradiation.[41] The deformation of the beam was obtained by measuring the change of the gap, δ, between the two gauges at A (see Figure 1b,c, (f1) and (f2)). For in situ heating of the sample during mechanical testing, the stage is resistively heated while the temperature is measured by a cofabricated bimetal type temperature sensor with a temperature measurement resolution of ±2 °C.[23,24] In our previous papers,[23,24] we experimentally calibrated the temperature difference between the stage and sample during Joule heating of the stage. Also, we showed that the SiC stage uniformly increases sample temperature. In the present manuscript, we used the same precalibrated SiC stage with known relationship between the sample temperature and applied voltage for accurate temperature measurement of the sample. Further details on the mechanical and thermal measurement of the MEMS stage can be found elsewhere.[23,24,29,30]

Although the stage offers a uniaxial testing mode,[23,24] we utilize the bending test to study size and temperature dependent plasticity in the SCS samples. Bending limits the high stress region to a small volume, and thus minimizes the likelihood of fracture due to flaws. Bending also increases the sample stress so that one can explore the possible onset of plasticity. For example, consider a simple cantilever beam loaded by a force, F, as shown in Figure 1e. For simplicity, we assume the cantilever beam is linear elastic, isotropic, and homogeneous, and the material deformation is small. It is easy to show that the stress state due to F is $\sigma(x, y) = F(L-x)y/I$ in the cantilever beam[31] where x and y are coordinates of the beam in the longitudinal and transverse directions, L and H are length and height of the beam, respectively, and I is a moment of inertia of the given cross section (see Figure 1e). In order to study the onset of plasticity at σ_{yield}, we may apply F during bending test such that material yields in a small volume in the vicinity of $x = 0$ and $y = \pm H/2$, while bending stress elsewhere is smaller than σ_{yield}. On the other hand, with uniaxial loading, the entire gauge length of the sample is subjected to σ_{yield} to induce material yield. Any flaw within the entire volume of the sample may cause fracture before the high σ_{yield} can be reached, giving the false impression that the material is brittle.

2.3. SCS Bending Samples

The SCS bending sample shown in Figure 1b is fabricated by lithography based microfabrication technology, and focused ion beam (FIB) milling followed by Freon (CF4) reactive ion etching (RIE) with an etching depth >100 nm. This additional RIE etching is to eliminate the effect of gallium ion bombardment on the mechanical properties of SCS. For example, it is well known that for silicon, the thickness of damaged layers due to gallium ion bombardment (i.e., formation of an amorphous layer at the surface) is around 20–30 nm, while the implantation depth of gallium ions is 40–56 nm at a beam energy of 30 keV.[32] In addition, we annealed the sample at >250 °C for 2 h to remove FIB induced point defects and defect clusters at the surface.[33,34] High precision milling by FIB also ensures the identical dimension of the eight bending arms for symmetric bending deformation of the sample. The crystal orientation of all bending arms along the longitudinal direction is <110> (see Figure 1c) with an elastic modulus of 169 GPa.[30]

It is worth noting that although the AFM based bending test is frequently used to characterize small scale materials due to its simplicity,[22,21] there may be stick-slip between an AFM tip and the bending arm during loading of a sample which makes data interpretation difficult. On the other hand, all bending arms in Figure 1c have well defined boundary conditions. Hence, the stress state of the bending sample can be evaluated from a force-displacement relationship. For example, we find a good agreement between experimental and predicted force-displacement relationship at room temperature. The difference in the slope of the $f-\delta$ in Figure 1d is within 1% for $h = 1.5$ μm. Further details on the analytical $f-\delta$ relationship can be found in the Supporting Information.

3. Results and Discussion

Here, we experimentally explore the size and temperature dependent BDT behavior by testing the SCS bending samples with widths varying from 720 nm to 8.7 μm. The depth of beams is between 6.5 and 8.7 μm. For each temperature, we heated the SiC stage by Joule heating and maintained the temperature for 20 min before any mechanical loading of the sample was applied. All experiments were carried out in a vacuum environment (<10^{-6} torr) to eliminate the effect of oxidation on the plastic deformation of SCS at high temperature.

3.1. Thermomechanical Response of SCS Bending Samples

The experimental f–δ relationship for $h = 720$ nm, 1.5 μm, and 8.7 μm are shown in **Figure 2**. In order to evaluate the stress state of the sample during the in situ experiment, we obtained the theoretical f–δ relationship (the dotted lines) and the corresponding maximum bending stress (σ_{max}) in the sample using linear elastic finite element analysis. We will discuss the σ_{max}–f relationship in further detail later. Note that the slope of the f–δ decreases with temperature due to reduction of the elastic modulus of SCS.[21,23,24,35,36]

The experimental f–δ response for $h = 1.5$ μm (Figure 2a) shows linear elastic behavior at 25, 184, and 293 °C. For each temperature, the sample was loaded and unloaded to check the reversibility and any permanent deformation. In all the three cases, we found a linear and reversible f–δ response for the strains applied. As temperature was increased to 340 °C, we observed yielding with 3.1 μm plastic displacement after removal of the mechanical load from the sample. In order to experimentally confirm the BDT behavior, we tested another sample with $h = 1.5$ μm again at 293 °C, and the sample failed (fractured) without any plastic deformation (see Figure 2a). The load-deformation relationship of the latter sample coincides with that of the former tested at 293 °C. Thus, for $h = 1.5$ μm, BDT occurs at a temperature between 293 and 340 °C.

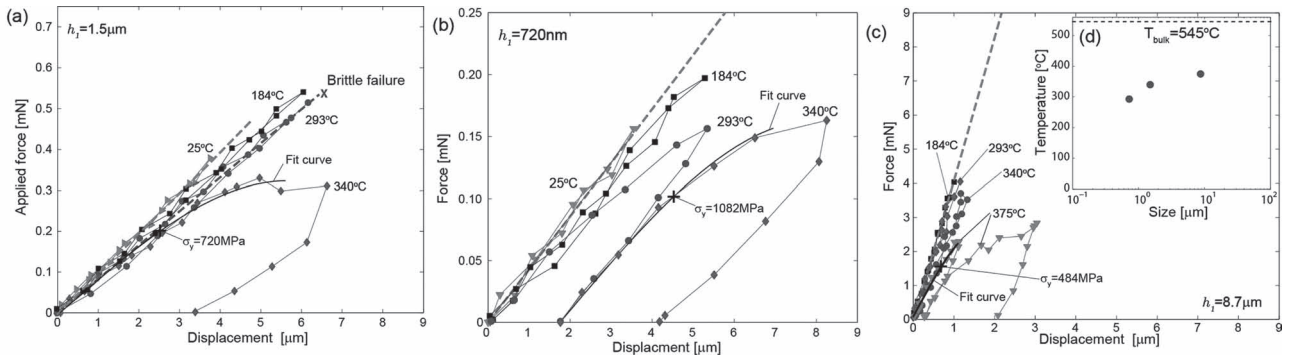

Figure 2. Force-displacement responses of single crystal silicon samples with variation of sample size and temperature: a) h = 1.5 μm; b) h = 720 nm; c) h = 8.7 μm. Note that the plasticity is observed at lower temperature with reduction of sample size, as summarized in (d). The σ_y is the maximum bending stress in the sample obtained by FEM analysis of the linear elastic deformation of the sample at f_{yield} when $df/d\delta = 0.8df/d\delta$ as f approaches zero.

To study the role of sample size on BDT, we used a smaller sample with h = 720 nm. From the f–δ response in Figure 2b, we observed linear elastic behavior at 25 and 184 °C. At 293 °C the sample deformed plastically with a 1.8 μm permanent deformation after unloading. Thus, the BDT temperature decreased with sample size. At higher temperature (340 °C), the 720 nm sample showed plastic deformation as expected (2.4 μm permanent deformation after the loading/unloading cycle). When sample size is larger (h = 8.7 μm; see Figure 2c), the f–δ response shows linear elastic behavior at 184, 293, and 340 °C during loading and unloading of the bending sample. At 375 °C, we measured 250 nm and 1.7 μm permanent deformations after the first and second loading/unloading cycles, respectively, i.e., the BDT temperature is between 340 and 375 °C. Note that the magnitude of plastic deformation depends on the applied strain during loading. Thus, the BDT temperature increases with sample size. The BDT temperature reduced by 21, 25, and 31% of the bulk BDT temperature[14] for samples with h = 8.7 μm, 1.5 μm, and 720 nm, respectively (see Figure 2d).

Figure 3 shows the SEM images of plastic deformation in the SCS bending samples. In Figure 3a, the initial configuration of the bending sample before any mechanical loading is shown (the zoom-in view of Area A is shown in Figure 3b). Figure 3c shows significant change in the sample configuration due to plastic deformation after complete removal of any mechanical loading. Figure 3d shows the zoom-in view of Area E in Figure 3e after ductile fracture of the SCS sample. Note that the permanent curvature with respect to the reference lines in Figure 3b,d clearly indicates substantial plastic deformation of the bending arms.

In order to compare the three experiments, we need to estimate the yield stress of the samples near the BDT. To do so, we used the experimental f–δ data; however, it is difficult to identify precisely the point on the f–δ curve when it deviates from linearity. In macroscopic uniaxial tests giving stress-strain data, often a criterion is used to determine yield stress, such as the stress at 0.2% offset strain. Here, we apply the criterion that the sample yields when the slope of the f–δ curve decreases to 80% of the initial value. We assume that silicon behaves as a linear elastic material up to this point, i.e., the most stressed point of the sample yields at the corresponding load. We fit the data to $f = a\delta + b\delta^3$ where a and b are fitting parameters. The fit model captures the experimental f–δ relationship well as the R^2 values (the coefficient of determination) for the least squares fitting curves in Figure 2a–c are 98.75, 99.28, and 99.84%, respectively. We find the yielding load, f_{yield}, at 0.1019, 0.2003, and 1.6769 mN for h = 720 nm, 1.5 μm, and 8.7 μm. The maximum stress in the sample at f_{yield} is obtained from a linear elastic finite element simulation using known elastic properties (Poissons ratio 0.28 and elastic modulus 169 GPa) of silicon. The analysis involves one-to-one scale solid model for the sample where sample dimensions are measured from the high resolution SEM images. The analysis gives σ_y = 1082, 720, and 484 MPa for h = 720 nm, 1.5 μm, and 8.7 μm, respectively, as shown in Figure 2. This result seems to suggest that yield strength of SCS samples under bending stress is size dependent although this issue is beyond the scope of the present paper.

3.2. Mechanism for Size and Temperature Dependent BDT

Our in situ experimental study indicates that BDT in SCS depends on sample size and temperature, as the BDT

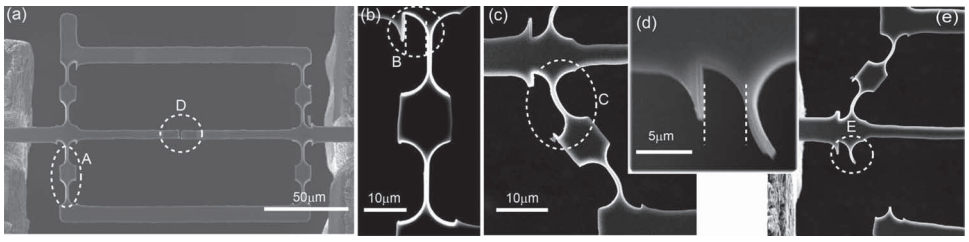

Figure 3. The SEM images of the SCS bending sample: a) initial configuration without any mechanical loading; b) zoom-in view of Area A in (a); c) plastic deformation of the bending arm after complete unloading of the sample; d) zoom-in view of Area B after material failure of the sample (also see E in (e)). Note that permanent curvature after failure in (d) indicates considerable plastic deformation (see the reference lines in (b) and (d)).

temperature decreases with sample size. Here, we propose a mechanism for the observed size and temperature dependent BDT in SCS. Small samples have low bulk dislocation densities, and rely on nucleation for plasticity. However, they have the virtue of having large surface to volume ratios. Surface dislocations require less energy to nucleate compared to that of the bulk, i.e., they can be nucleated at lower temperatures compared with bulk nucleation. Smaller samples can thus lower their BDT temperature by nucleating large proportion of dislocations from free surfaces. As the size increases, the surface to volume ratio decreases, and the reliance on surface dislocation for plasticity decreases. Consequently, the BDT temperature increases, reaching a steady value.

With a reduction of sample size, surface effects become increasingly important as the surface-to-volume ratio is inversely proportional to the characteristic length scale of the sample size. Hence for small samples, dislocations are strongly influenced by nearby surfaces and interfaces. Dislocations move towards free surfaces and escape to minimize the stress and strain energy of the crystal, i.e., they are subjected to attractive image forces from the surface. The image force is inversely proportional to the distance from the free surface.[37] Hence, self-energy or the strain energy of the crystal induced by a single dislocation near free surfaces can be substantially lower than the energy due to a dislocation in the bulk.[38] Thus, introduction of a dislocation near the free surface is likely to be energetically less expensive than that in a large crystal. For example, Shuch et al. experimentally found, using nanoindentation, that the energy to nucleate a surface dislocation in single crystal platinum is 0.28 eV, whereas the corresponding bulk value is 1.3 eV.[39] Several MD simulation results of small scale SCS samples show that the surface serves as a source of dislocations in small samples.[40,42,43] Kang and Cai predicted that SCS can plastically deform at room temperature by dislocation initiated from surface when sample size is less than 4 nm.[40] In addition, the number of preexisting defects including dislocations in a sample is proportional to the volume of the sample, and thus rapidly reduces with sample size. For semiconductive materials like SCS with extremely low defect densities, nanometer or even micrometer-sized samples can have only a few or no preexisting dislocations.[37] Hence, the onset of plasticity is likely controlled by surface dislocation nucleation rather than dislocation multiplication from preexisting dislocations.

Consider a material sample with perfect crystal structure. The sample is in thermodynamic equilibrium and the probability density of an atom at a specific position in the crystal structure is given by Boltzmann distribution at temperature, T.[44] With an increase in thermal energy in the crystal, thermal vibration of the atom becomes larger and hence the probability of having an atom with higher energy state increases in the system. When the thermal energy is sufficiently large, there is the possibility of having an atom jump out of the lattice and nucleate a dislocation. Let the activation energy of dislocation nucleation be U. Then, the rate at which dislocation nucleates per unit volume at absolute temperature, T, is given by $\dot{n} = f\exp(-U/kT)$, where k is the Boltzmann constant and f is a constant.[44] Thus, for SCS, one expects that as the temperature approaches a critical temperature, there will be an abundance of dislocations which will facilitate plasticity. Below this temperature, not only is the dislocation nucleation rate low, but also the dislocation glide of existing dislocations is limited due to high Peierls stress.[14] An external stress on the sample facilitates the nucleation of dislocation, i.e., reduces the energy barrier for nucleation. Let $U–F^*$ be the remaining barrier due to a given applied stress on the sample. Then, the nucleation rate per volume changes to $\dot{n} = f\exp(-(U–F^*)/kT)$.

The dislocation nucleation rate equation indicates that the BDT temperature reduction, i.e., sufficiently large $\dot{n}$ at lower temperature $T < T_{BDT}$ (T_{BDT} is bulk BDT temperature), can be achieved by either a decrease in the remaining barrier ($U–F^*$) with larger F^* or a decrease in U. For bulk SCS, fracture occurs before silicon yields unless the BDT temperature is reached. As the size decreases, a decrease in the BDT temperature implies one or both of the following possibilities: (1) U decreases with size, and/or (2) U remains the same but F^* can be increased, i.e., stress can be increased without fracture. The latter implies that brittle fracture strength increases with decreasing sample size. We observed experimentally that at a given temperature lower than the bulk BDT temperature, smaller silicon samples yield but larger samples fractures in a brittle manner (at 293 °C, a 1.5 μm sample fractures at 2 GPa (Figure 2a), but a 720 nm sample yields at 1.082 GPa (Figure 2b). This observation is only possible if U decreases with sample size. The characteristics of atoms at the surface and in the bulk may be substantially different due to surface effects. With decreasing sample size, the effect of the surface becomes more important as the surface-to-volume ratio increases and thus U may decrease although the phonon and atom vibrations in bulk Si may not change. Thus, we will consider a mechanism for size dependent BDT temperature that involves a decrease in U due to stronger surface effects.

Consider surface and volume dislocation nucleation in a cylindrical SCS sample shown in **Figure 4**a at a given temperature, T. The length and diameter of the sample are l and $d(= 2R)$, respectively, and r is a radial coordinate of the sample at its cross section. Suppose the surface effects become fully dominant within a small interval, $R > r > R–\alpha a$, where a is the length of the crystalline unit cell and α is a constant representing a number of unit cells. Since dislocation nucleation from the surface requires less energy as discussed earlier, we introduce the dislocation nucleation rate from the surface with activation energy, U_S. Hence, the dislocation nucleation rate in the bulk volume ($\dot{n}_V$) and at surface ($\dot{n}_S$) can be written as follows

$$\left.\begin{array}{l} \dot{n}_V = f_V\exp(-\frac{U_V}{kT})\left[s^{-1}m^{-3}\right],\ R-\alpha a > r > 0 \\ \dot{n}_S = f_S\exp(-\frac{U_S}{kT})\left[s^{-1}m^{-3}\right],\ R > r > R-\alpha a \end{array}\right\} \quad (1)$$

where f_V and f_S are constants, and $U_V > U_S$ are activation energies from bulk volume (V) and surface (S), respectively. The total dislocation nucleation rate in a given volume $V_T = \pi R^2 l$ becomes $\dot{N}_{TOT} = V_V\dot{n}_V + V_S\dot{n}_S$ where $V_V = (R-\alpha a)^2\pi l$ and $V_S = V_T–V_V$ (see Figure 4a). The corresponding dislocation nucleation rate per volume ($= \dot{N}_{TOT}/V_T$) is

$$\dot{n}_{TOT} = \left(1-\frac{\alpha a}{R}\right)^2\dot{n}_V + \left(2\frac{\alpha a}{R} - \left(\frac{\alpha a}{R}\right)^2\right)\dot{n}_S \quad (2)$$

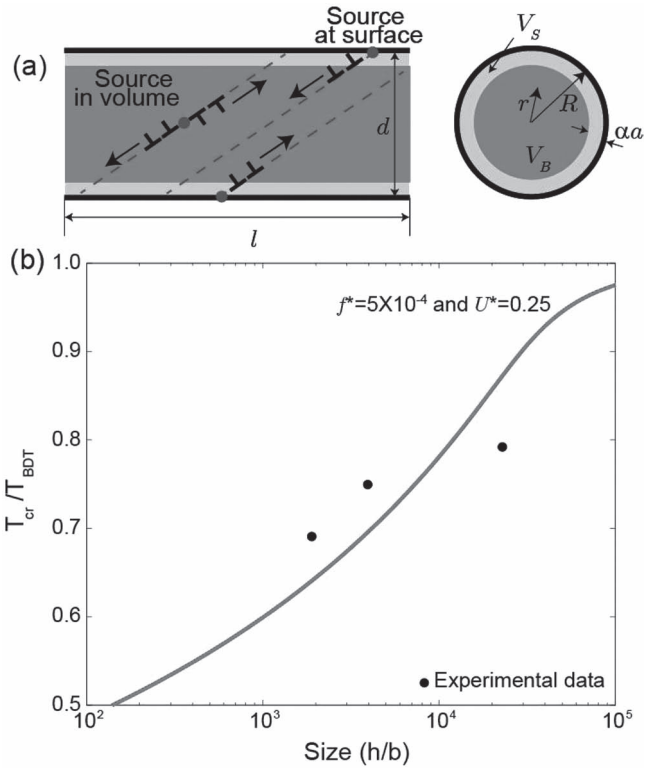

Figure 4. Mechanism for size and temperature dependent brittle-to-ductile transition (BDT) in silicon: a) the schematic of the dislocation nucleation from the sources in the bulk volume and at the surface and b) theoretical predictions of the size dependent BDT temperature.

For bulk materials ($R \gg \alpha a$), Equation 2 gives $\dot{n}_{TOT} \to \dot{n}_V$ due to weak surface effects while $\dot{n}_{TOT}$ converges to $\dot{n}_S$ with $R \to \alpha a$ as the surface effects become dominant.

For qualitative prediction of BDT temperature reduction with sample size, let $\dot{n}_{BDT}$ be the nucleation rate at BDT in bulk SCS at T_{BDT}. If $\dot{n}_{BDT}$ is a necessary and sufficient condition for the BDT at all size scales, then one expects that the BDT temperature would decrease with size. The qualitative nature of this decrease can be revealed by equating $\dot{n}_{TOT}$ at T in Equation 2 to $\dot{n}_{BDT}$ for bulk, i.e., equating $f_{\mathrm{V}} \exp(-U_{\mathrm{V}}/kT_{\mathrm{BDT}})$ with the right side of Equation 2. This gives

$$\frac{1}{\exp(-\beta)}\left((1-a^*)\exp\left(\frac{-\beta}{T^*}\right)+(2-a^*)\,a^* f^* \exp\left(\frac{-U^*\beta}{T^*}\right)\right)=1 \quad (3)$$

where $a^* = \alpha a/R$, $f^* = f_{\mathrm{S}}/f_{\mathrm{V}}$, $U^* = U_{\mathrm{S}}/U_{\mathrm{V}}$, $T^* = T/T_{\mathrm{BDT}}$, and $\beta = U_{\mathrm{V}}/kT_{\mathrm{BDT}}$. Equation 3 predicts an upper and a lower bound of BDT temperatures as a function of size. For large sizes ($a^* \to 0$), $T \to T_{\mathrm{BDT}}$ (bulk). For small sizes ($a^* \to 1$), $T/T_{\mathrm{BDT}} \to U^*\beta/(\beta - \exp(1/f^*))$ which becomes a function of the material's properties. Using Equation 3 and a well known value for the BDT in bulk SCS ($\beta = 23.71$),[14] the BDT temperature trend is shown in Figure 4b as a function of sample size where values of f^* and U^* are chosen such that the model prediction closely matches with experimental observations. As experimentally observed in Figure 2d, the BDT temperature gradually decreases with sample size due to stronger surface effects. Although our proposed model captures the qualitative behavior of the observed size and temperature dependent BDT, further characterization of U_{S} and f_{S} is required for quantitative prediction of the size dependent BDT behavior for SCS.

4. Summary

We carried out quantitative, in situ thermo-mechanical tests of silicon crystal silicon, revealing that the onset of plasticity depends on temperature and sample size. A 31% reduction in the BDT temperature was observed in the silicon crystal silicon with respect to bulk silicon. A likely mechanism for this decrease in temperature with size is the relatively low energy demand for dislocation generation from the free surface compared to that from within the bulk. As size decreases, the surface to volume ratio increases. Thus, the free surface becomes the dominant source of dislocations necessary to initiate plasticity at lower temperature. We developed a model representing this mechanism, which qualitatively predicts the experimental observations. The work provides useful insight for the design and reliable analysis of micrometer and nanometer scale devices involving single crystal silicon operating at room to high temperatures.

Supporting Information

Supporting Information is available from the Wiley Online Library or from the author.

Acknowledgements

This research was funded by NSF ECCS 11-02201. The single crystal silicon samples were fabricated in Micro-Nano-Mechanical-Systems Laboratory at the University of Illinois at Urbana-Champaign. The tensile testing was performed in Frederick Seitz Materials Research Laboratory and Beckman Institute for Advanced Science and Technology at UIUC.

Received: July 16, 2012
Revised: August 15, 2012
Published online: September 7, 2012

[1] S. S. Brenner, *J. Appl. Phys.* **1956**, *27*, 1484.
[2] S. S. Brenner, *J. Appl. Phys.* **1957**, *28*, 1023.
[3] E. O. Hall, *Proc. Phys. Soc., London, Sect. B* **1951**, *64*, 747.
[4] N. J. Petch, *J. Iron Steel Inst.* **1953**, *174*, 25.
[5] W. D. Nix, H. Gao, *J. Mech. Phys. Solids* **1998**, *46*, 411.
[6] J. Rajagopalan, J. H. Han, M. T. A. Saif, *Science* **2007**, *315*, 1831.
[7] W. D. Nix, J. R. Greet, G. Feng, E. T. Lilleodden, *Thin Solid Films* **2007**, *515*, 3152.
[8] S. H. Oh, M. Legros, D. Kiener, G. Dehm, *Nat. Mater.* **2009**, *8*, 95.
[9] J. Stolken, A. Evans, *Acta Mater.* **1998**, *46*, 5109.
[10] N. Fleck, G. Muller, M. Ashby, J. Hutchinson, *Acta Metall. Mater.* **1994**, *42*, 475.
[11] S. Ashley, *Mech. Eng.* **1997**, *119*, 78.
[12] A. H. Epstein, *Aerosp. Am.* **2000**, *38*, 30.
[13] M. A. Fonseca, J. M. English, M. von Arx, M. G. Allen, *J. Microelectromech. Syst.* **2002**, *11*, 337.

[14] J. Samuels, S. G. Roberts, *Proc. R. Soc. London, Ser. A* **1989**, *421*, 1.
[15] C. S. John, *Philos. Mag.* **1975**, *32*, 1193.
[16] J. F. Knott, *Fundam. Fract. Mech.* **1973**.
[17] S. Nakao, T. Ando, M. Shikida, K. Sato, *J. Micromech. Microeng.* **2008**, *18*, 015026.
[18] X. D. Han, *Nano Lett.* **2007**, *7*, 452.
[19] F. Östlund, *Adv. Funct. Mater.* **2009**, *19*, 2439.
[20] Y. Zhu, F. Xu, Q. Q. Qin, W. Y. Fung, W. Lu, *Nano Lett.* **2009**, *9*, 3934.
[21] T. Namazu, Y. Isono, T. Tanaka, *J. Microelectromech. Syst.* **2000**, *9*, 450.
[22] S. Hoffmann, *Nano Lett.* **2006**, *6*, 622.
[23] W. Kang, M. Saif, *MRS Commun.* **2011**, *1*, 13.
[24] W. Kang, M. Saif, *J. Micromech. Microeng.* **2011**, *21*, 105017.
[25] M. A. Haque, M. T. A. Saif, *Proc. Natl. Acad. Sci. USA* **2004**, *101*, 6335.
[26] M. D. Uchic, D. M. Dimiduk, J. N. Florando, W. D. Nix, *Science* **2004**, *305*, 986.
[27] Y. Zhu, H. D. Espinosa, *Proc. Natl. Acad. Sci. USA* **2005**, *102*, 14503.
[28] D. Kiener, W. Grosinger, G. Dehm, R. Pippan, *Acta Mater.* **2008**. *56*, 580.
[29] W. Kang, M. T. Saif, *J. Microelectromech. Syst.* **2010**, *19*, 1309.
[30] W. Kang, J. H. Han, M. T. Saif, *J. Microelectromech. Syst.* **2010**, *19*, 1322.
[31] S. Timoshenko, *Theory of Elasticity*, 3rd Ed, McGraw-Hill Publishing Company, New York **1970**.
[32] S. Rubanov, P. R. Munroe, *J. Microsc. (Oxford)* **2004**, *214*, 213.
[33] O. W. Holland, M. K. El-Ghor, C. W. White, *Appl. Phys. Lett.* **1988**, *53*, 1282.
[34] J. W. Corbett, J. P. Karins, T. Y. Tan, *Nucl. Instrum. Methods.* **1981**, *182–183*, 457.
[35] T. Yi, L. Li, C. J. Kim, *Sens. Actuators, A* **2000**, *83*, 172.
[36] T. Tsuchiya, *J. Microelectromech. Syst.* **2005**, *14*, 1178.
[37] D. Hull, D. J. Bacon, *Introduction to Dislocations*, 3th Ed, Oxford University Press, New York **1984**.
[38] P. Khanikar, A. Kumar, A. Subramaniam, *Philos. Mag.* **2011**, *91*, 730.
[39] C. A. Schuh, J. K. Mason, A. C. Lund, *Nat. Mater.* **2005**, *4*, 617.
[40] K. W. Kang, W. Cai, *Int. J. Plast.* **2010**, *26*, 1387.
[41] J. Zang, L. Bao, R. A. Webb, X. Li, *Nano Lett.* **2011**, *11*, 4885.
[42] J. Guenole, J. Godet, S. Brochard, *Model Simul. Mater. Sci. Eng.* **2011**, *19*, 074003.
[43] Z. Yang, Z. Lu, Y. Zhao, *J. Appl. Phys.* **2009**, *106*, 023537.
[44] V. Bulatov, W. Cai, *Computer Simulations of Dislocations*, Oxford University Press, New York **2006**.